Supporting Information to Accompany "**A red emissive two-photon fluorescent probe for mitochondrial sodium ions imaging in live tissue**"

Vinayak Juvekar,[a] Myoung Ki Cho,[a] Hyo Won Lee,[a] Dong Joon Lee,[a] Ju Man Song,[b] Jong Tae Je*[b] and Hwan Myung Kim*[a]

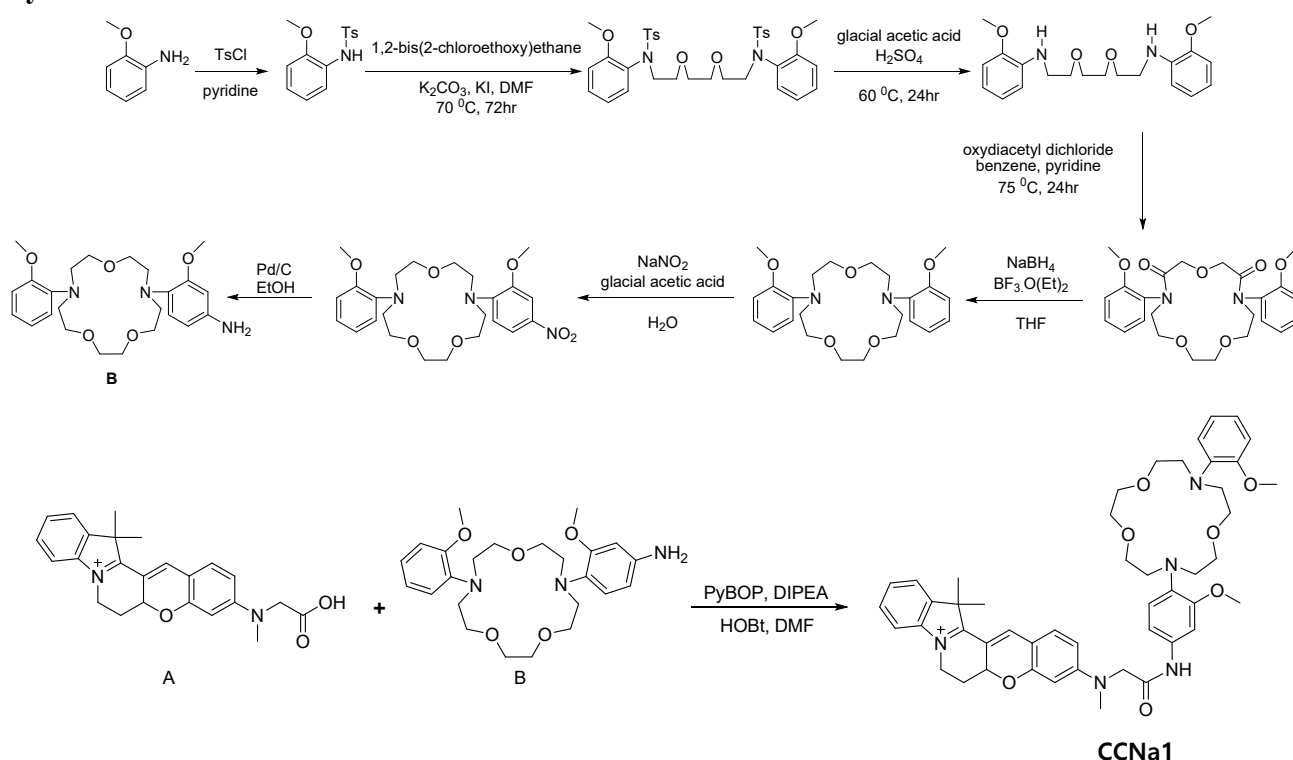*[a]Department of Energy Systems Research and Department of Chemistry, Ajou University, Suwon 443-749, South Korea. Email: kimhm@ajou.ac.kr*

[b]Giheung R&D Center, SFC Co., Ltd., Yongin, 16953, South Korea. Email: jtje@sfc-dye.com

Table of Contents

Synthesis of CCNa1.

Compound **(A)** was received from SFC. Co. Ltd.,   and *N*-(2-methoxyphenyl)-*N'*-(4-amino-2-methoxyphenyl)-1,7-diaza-15-crown-5 **(B)** was prepared from following reported method.[1]

Probe **CCNa1**: The probe **CCNa1** was synthesized using compound **A** (0.13 g, 0.34 mmol) and compound **B** (0.15 g, 0.34 mmol) that were dissolved in anhydrous DMF (0.01 M, 30 ml). Further, hydroxybenzotriazole (HOBt, 0.13 g, 1.02 mmol) and N,N-diisopropylethylamine (0.1 mL) were also added and allowed to stir for 10 min under nitrogen atmosphere. Next, benzotriazol-1-yl-oxytripyrrolidinophosphonium hexafluorophosphate (PyBOP, 0.53 g, 1.02 mmol) was added to the reaction mixture and continued stirring for 36 h at room temperature (rt). The solvent was evaporated in vacuo and the residue was dissolved in CHCl$_3$ (15 ml), washed thrice with DW. The organic layer was dried over MgSO$_4$ and evaporated to obtain the crude product which was purified by silica column chromatography using CHCl$_3$/MeOH (9.7:0.3 to 9.3:0.7) to give **CCNa1** as a violet solid 0.15g (54%). MP was 175-180 °C; ^{1}H NMR (400 MHz, d6-DMSO): δ 10.07 (s, 1H), 8.27 (s, 1H), 7.74 (dd, *J* = 0.8, 7.2 Hz, 1H), 7.64 (d, *J* = 7.6 Hz, 1H), 7.54 – 7.44 (m, 3H), 7.34 (d, *J* = 2.0 Hz, 1H), 7.04 –   6.95(m, 3H), 6.91 (d, *J* = 1.8 Hz, 2H), 6.86 – 6.81 (m, 1H), 6.59 (dd, *J* = 2.8, 9.2 Hz, 1H), 6.27 (d, *J* = 2.4 Hz, 1H), 5.33 – 5.29 (m, 1H), 4.55 (dd, *J* = 4.0, 13.2 Hz,1H), 4.35 (s, 2H), 4.14 – 4.08 (m, 1H), 3.72 (d, *J* = 9.2 Hz, 6H), 3.55 – 3.51 (m, 8H), 3.47 – 3.45 (m, 5H), 3.28 – 3.23 (m, 8H), 3.20 – 3.17 (m, 4H), 2.72-2.68(m, 2H), 1.94(d, J = 13.6 Hz, 1H) 1.81(s, 3H), 1.68(s, 1H). ^{13}C NMR (100 MHz, d6-DMSO):177.6, 173.6, 166.1, 166.0, 158.9, 156.3, 152.8 142.3, 142.2, 140.7, 139.8, 128.5, 127.5,

122.5, 120.6, 113.0, 112.1, 110.2, 108.3, 97.8, 70.4, 69.8, 68.5, 55.4, 55.3, 53.2, 50.5, 29.1, 26.6, 25.4; HRMS (FAB$^+$): m/z calcd for [C$_{48}$H$_{58}$N$_5$O$_7$]: 817.0029, found: 816.4340

Water Solubility of CCNa1 in MOPS buffer. The stock solution of **CCNa1** (1.0×10^{-2} M) was prepared in DMSO and diluted to ($1.0 \times 10^{-5} \sim 1.0 \times 10^{-7}$) M with 3.0 ml of MOPS buffer (10 mM, pH 7.0) in a standard cuvette. The total concentration of DMSO in DW was maintained at 0.1 % in all samples.[2] A hyperbolic curve was observed in the plot of fluorescence intensity v/s the concentration of the dye (Figure S2). The maximum concentration in the linear region was taken as the solubility. The maximum solubility of **CCNa1** in MOPS buffer was determined to be 5 μM.
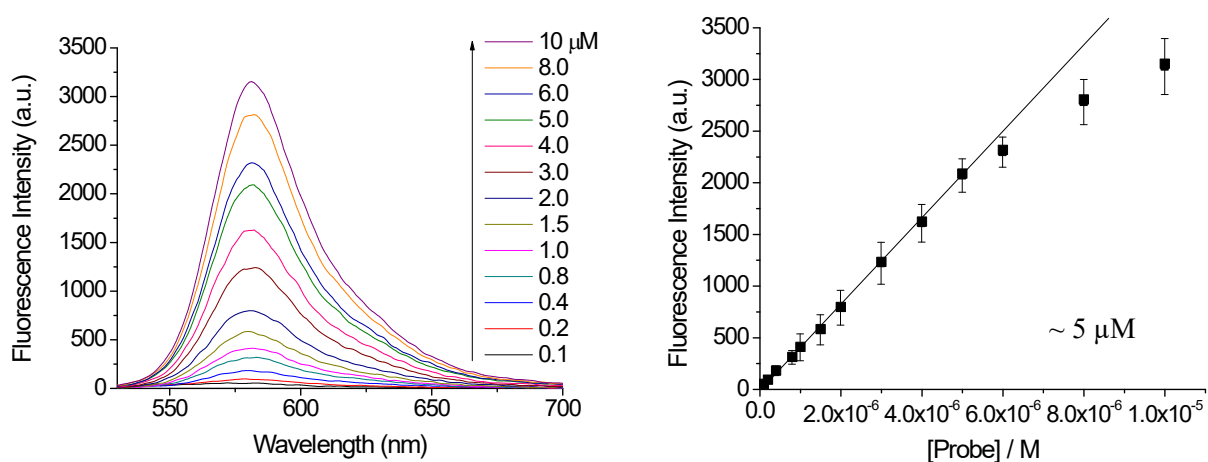
Figure S1. (a) One-photon fluorescence spectra and (b) plot of fluorescence intensity v/s the concentration of **CCNa1** in 3.0 mL MOPS buffer (pH 7.0). The emission spectra were recorded with λ_{Ex} = 530 nm.

Spectroscopic measurements of CCNa1. Absorption spectra and fluorescence spectra were measured in a standard quartz cell (1 cm) with the S-3100 UV-Vis spectrophotometer and FluoroMate FS-2 fluorescence spectrophotometer, respectively.
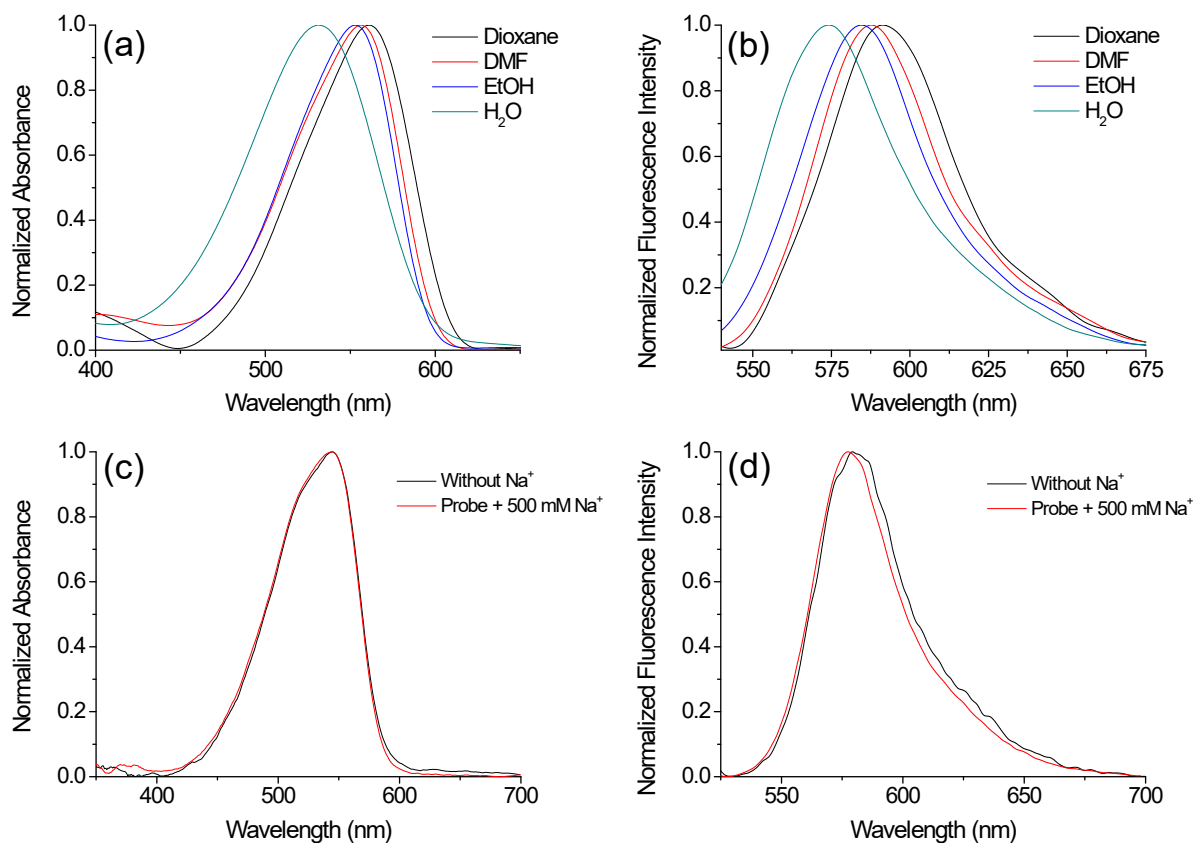

Figure S2. Normalized absorption (a) and emission (b) spectra of **CCNa1** in 1,4-dioxane, DMF, EtOH and buffer (10 mM MOPS, pH 7.0). Normalized absorption (c) and emission (d) of **CCNa1** in absence and presence of excess Na^+ (500 mM) in MOPS buffer (10 mM MOPS, pH 7.0). The emission spectra were recorded with λ_{Ex} = 530 nm.

Table S1. Absorption and emission maxima of **CCNa1** recorded in different solvents.

| Solvent(E^N_T) [a]	$\lambda_{Ex\,(max)}$, nm[b]	λ^{fl}_{max}, nm[c]
1,4-Dioxane (0.164)	562	591
DMF (0.386)	558	588
EtOH (0.654)	554	585
buffer (1.000)[d]	537	575

(a) The normalized empirical parameter of solvent polarity are presented parenthesis.[3]   (b) The one-photon absorption $\lambda_{Ex\,(max)}$ nm and (c) the emission spectra λ^{fl}_{max} nm. d) 10 mM MOPS buffer (pH 7.0). The E^N_T value is for water.
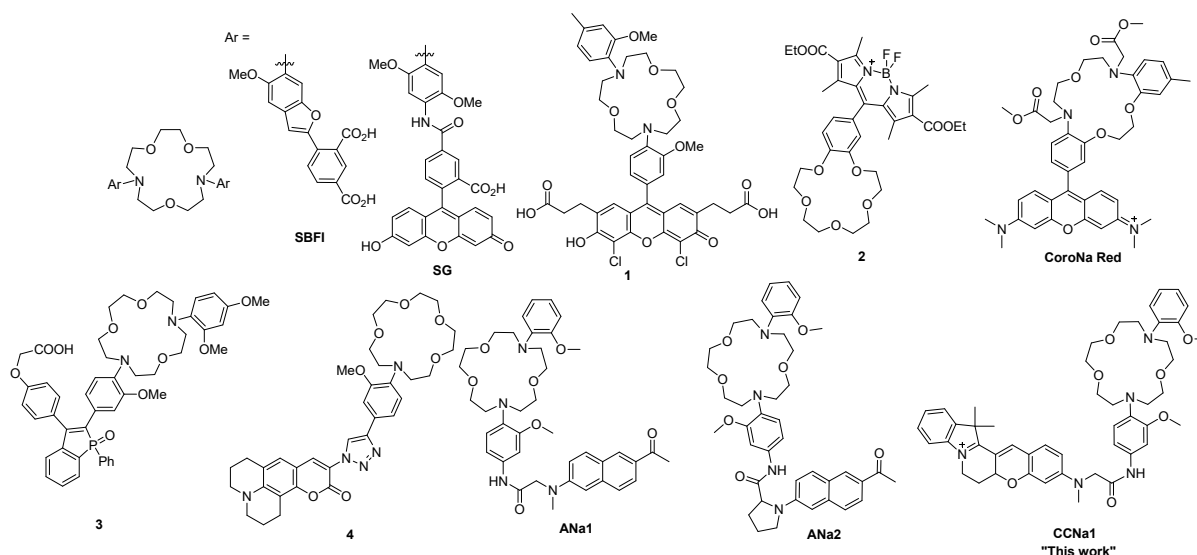
Chart S1. Representative small molecule Na$^+$ ion probe structures.

Table S2. Photophysical properties of **Na$^+$** ion probes.

Compound[a]	$\lambda_{max}^{(1)}/\lambda_{max}^{fl}$ [b]	Φ[c]	$K_d^{Na(d)}/K_d^{Na/K}$ [e]	K_d^{K} [f]	FEF_{Na}[g]	$\delta\Phi$ [h] [$\lambda_{max}^{(2)}$] [i]	Ref.
SBFI	346/551	0.045				n.a	4,5
SBFI+Na$^+$	334/525	0.083	3.8/11	68	n.a	20 [780 nm]	
SG$^+$	n.a	n.a				n.a	6,5
SG+Na$^+$	507/532	0.2	6.0/21	246	7	30 [800 nm]	
1	517/542	0.014				0.45 [780 nm]	7
1+Na$^+$	517/542	0.20	8.3/34	n.a	13	5.91 [780 nm]	
2[j]	497/507	0.0027				n.a	8

Compound	$\lambda_{ex}/\lambda_{em}$	Φ	K_d^{Na}/$K_d^{Na/K}$	K_d^{K}	FEF	Two-photon	Ref
2+Na$^{+(j)}$	498/508	0.1	n.a	n.a	37(6.6)	n.a	
CoroNa Red	551/576	n.a				n.a	
CoroNa Red +Na$^+$	551/576	n.a	219/n.a	460	18	n.a	9
3	394/656	0.016				n.a	
3+Na$^+$	371/620	0.028	16/n.a	223	---	n.a	10
4	440/517	0.025				n.a	
4+Na$^+$	440/517	0.275	48	68	10.9(2.7)	n.a	11
ANa1	367/500	0.08				n.d^k	
ANa1+Na$^+$	367/500	0.65	8.0/20	280	8	95 [780 nm]	5
ANa2	366/500	0.023				3 [750 nm]	
ANa2+Na$^+$	366/500	0.35	18/21.6	296	15	83 [750 nm]	12
CCNa1	544/579	0.04				8 [740 nm]	
CCNa1+Na$^+$	545/577	0.34	21.7/22.2	n.d^k	9	83 [730 nm]	This Work

(a) See **Chart S1** in the ESI for the chemical structure. (b) All data were measured in aqueous solution. (c) Fluorescence quantum yield. (d) Dissociation constants for Na$^+$ in mM measured by one-photon processes in the absence (K_d^{Na}) and (e) presence ($K_d^{Na/K}$) of K$^+$ ([Na$^+$] + [K$^+$] = 135 mM). (f) Dissociation constants for K$^+$ in mM. (g) Fluorescence enhancement factor, $(F - F_{mim})/F_{min}$ probe towards Na$^+$ and the number in the parenthesis is the *FEF* of probe towards K$^+$. (h) Two-photon action cross section in 10^{-50} cm^{4}s/photon (GM). (i) λ_{max} of the two-photon excitation spectra in nm. (j) data was measured in methanol. (k) Data not determined (n.d) due to very weak optical output. n.a = data not available.
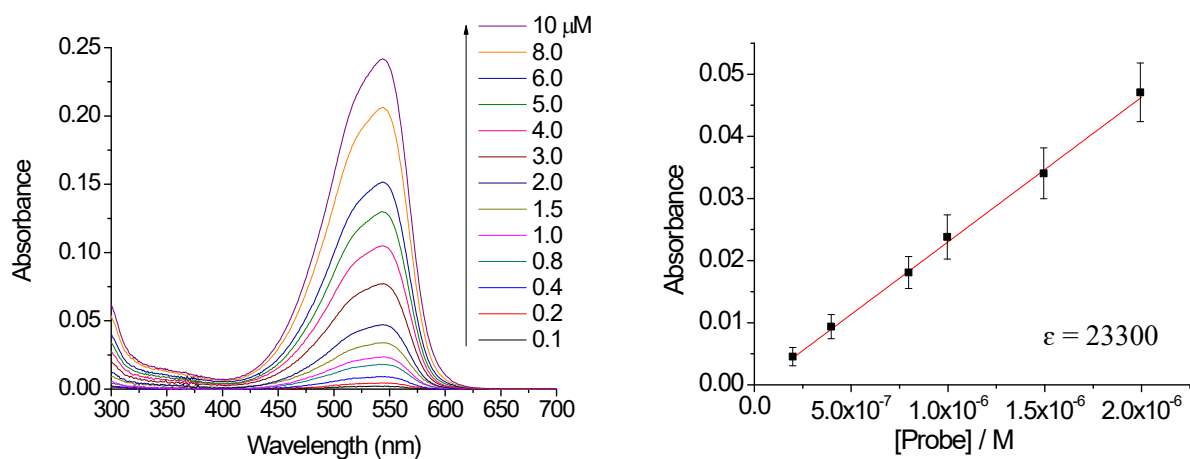
Figure S3. (a) Absorbance spectra and (b) plot of absorbance intensity against **CCNa1** in 3.0 mL MOPS buffer (pH 7.0).

Computational Method

Quantum mechanical calculations of CCNa1 and CCNa1-Na$^+$ were done using Gaussian 09 software package.[13] Ground state geometries were optimized at CAM-B3LYP/6-31G(d) level of theory, and excited state energies and geometries were calculated at TD CAM-B3LYP/6-31G(d) level of theory. From the results of excited state calculation, natural transition orbitals (NTO)[14] were generated using Gaussian 09 and visualized with GaussView 5.[15] It was shown that B3LYP/6-31G(d) can successfully describe the electronic transitions of fluorescent probes.[16] In addition, CAM-B3LYP[17] functional was used to account for the dispersion interaction in CCNa1.

Figure S4a and S4b show the electronic transitions of CCNa1 and CCNa1-Na$^+$ at ground-state optimized geometry on the left-hand side and at S_1-state optimized geometry on the right-hand side, together with the NTOs involved in each transition. The electronic transition at the ground-state optimized geometry corresponds to vertical transition from the ground state minimum i.e., absorption maximum of the electronic band. In condensed phase, electronically excited states relax to the vibrational ground level of the S_1 state (Kasha's rule) and emits from there. Therefore, the electronic transition at the S_1-state optimized geometry represents emission maximum of the fluorescence.

There are low-lying charge transfer (electron transfer) states, S_1 and S_2, of CCNa1 in Figure S4a. Charge (electron) is transferred from Na$^+$ receptor to the hemicyanine core. Due to low overlap of orbitals involved in the transitions, oscillator strengths for both S_1 and S_2 are very low. S_3 state has high oscillator strength and is responsible for the visible absorption. The electronically excited S_3 state undergoes IC to S_1 state, but fluorescence quantum yield from the S_1 state is very low with low oscillator strength due to its charge transfer nature. Fluorescence is turned off in bare CCNa1.

In the sodiated complex, CCNa1-Na$^+$, S_1 state results from a localized transition within the hemicyanine core, as shown in Figure S4b. S_2 state has a charge transfer character with zero oscillator strength, and does not contribute to UV-visible absorption. Emission from the S_1 state of CCNa1-Na$^+$ has a very high oscillator strength because the transition is also localized within the hemicyanine core. Therefore, one can expect bright fluorescence from the sodium complex i.e., fluorescence is turned on when CCNa1 captures a sodium ion.
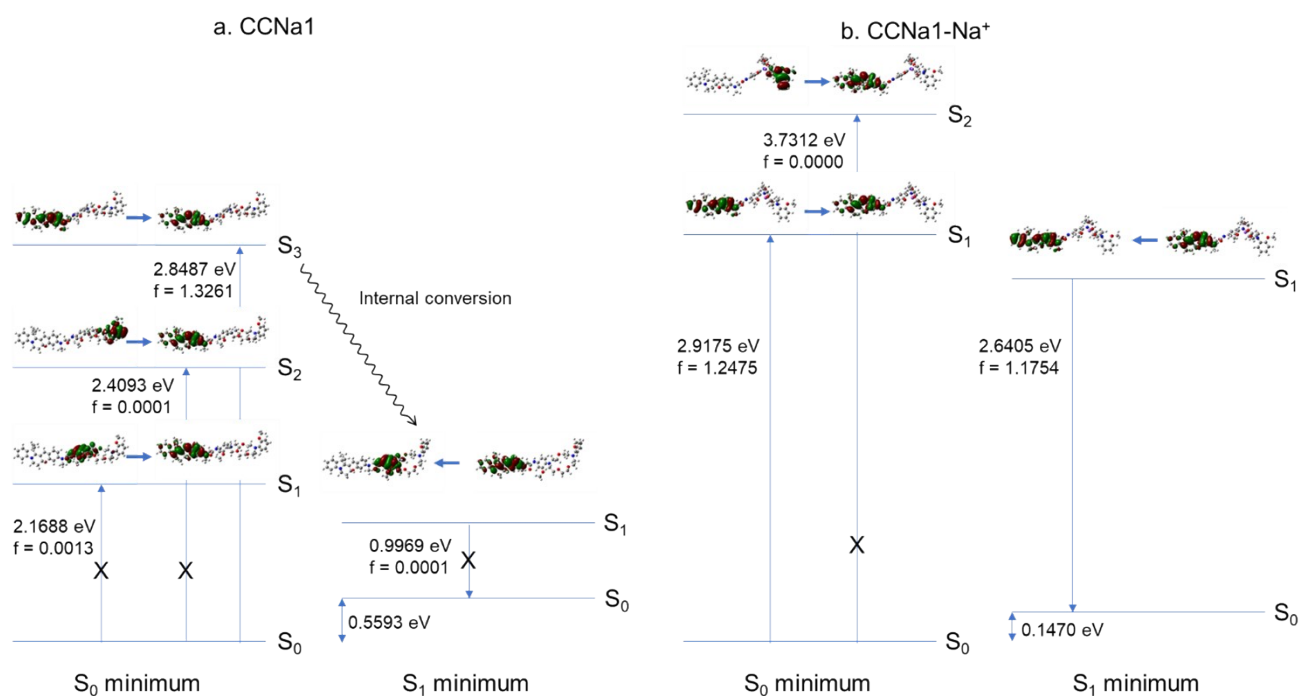
Figure S4. Electronic states, transition energy, oscillator strength, and natural transition orbitals of; a. CCNa1 and b. CCNa1-Na$^+$, calculated at TD-CAM-B3LYP/6-31G(d) level of theory.

Determination of Dissociation Constant: Solutions containing 1 μM **CCNa1**, 10 mM MOPS (pH 7.0) *solution A*: with 135 mM KCl and *solution B*: with 500 mM NaCl were prepared. A series of calibration solutions containing various [Na$^+$] was prepared by mixing two solutions in various ratios.[18]

Inorder tp determine the K_d for **CCNa1**-Na$^+$, the fluorescence spectrum was recorded with 3.0 mL of *solution A* (0 μM free Na$^+$) at 20 °C. Then 8 μL of this solution was discarded and replaced by 8 μL of *solution B*, and the spectrum was recorded. This would make the [Na$^+$] to 1.35 mM with no change in the probe concentration. Following titerations attained 2.70, 8.10, 10.8, 16.2, 27.0, 35.1, 43.2, 54.0, 94.5, 135.0, 250.0, 350.0, 450.0 and 500.0 mM free Na$^+$ by successively discarding 0.016, 0.048, 0.064, 0.097, 0.162, 0.216, 0.259, 0.324, 0.567, 0.810, 1.5, 2.1, 2.7 and 3.0 mL of *solution A,* respectively, and replacing each with an equal volume of *solution B*.

When a 1:1 metal-ligand complex is formed between probe and Na$^+$, one can describe the equilibrium as follows, where L and M represent probe and Na$^+$, respectively.

The total probe and metal ion concentration are defined as $[L]_0 = [L] + [LM]$ and $[M]_0 = [M] + [LM]$, respectively. With $[L]_0$ and $[M]_0$, the value of K_d is given by:

$$[LM]^2 - ([L]_0 + [M]_0 + K_d)[LM] + [L]_0[M]_0 = 0,$$

$$[LM] = \left\{([L]_0 + [M]_0 + K_d) - (([L]_0 + [M]_0 + K_d)^2 - 4[L]_0[M]_0)^{1/2}\right\}/2 \quad \ldots\ldots\ldots\ldots(1)$$

or $(F - F_{min}) = \left[\{([L]_0 + [M]_0 + K_d) - (([L]_0 + [M]_0 + K_d)^2 - 4[L]_0[M]_0)^{1/2}\}/2[L]_0\right](F_{max} - F_{min})$ ..(2)

where F is the observed fluorescence intensity, F_{min} is the minimum fluorescence intensity, and F_{max} is the maximum fluorescence intensity. The K_d value that best fits the titration curve (Figures S3, c) with Eq 2 was calculated by using the Excel program as reported.[19]

In order to determine the K_d^{TP} for the two-photon process, the TPEF intensity were recorded in the range of 450-550 nm with a DM IRE2 Microscope (Leica) excited by a mode-locked titanium-sapphire laser source (Mai Tai HP; Spectra Physics, 80 MHz pulse frequency, 100 fs pulse width) set at wavelength 750 nm and output power 2510 mW, which corresponded to approximately 10 mW average power in the focal plane. The TPEF titration curves (Figures S3c) were obtained and fitted Eq.2.
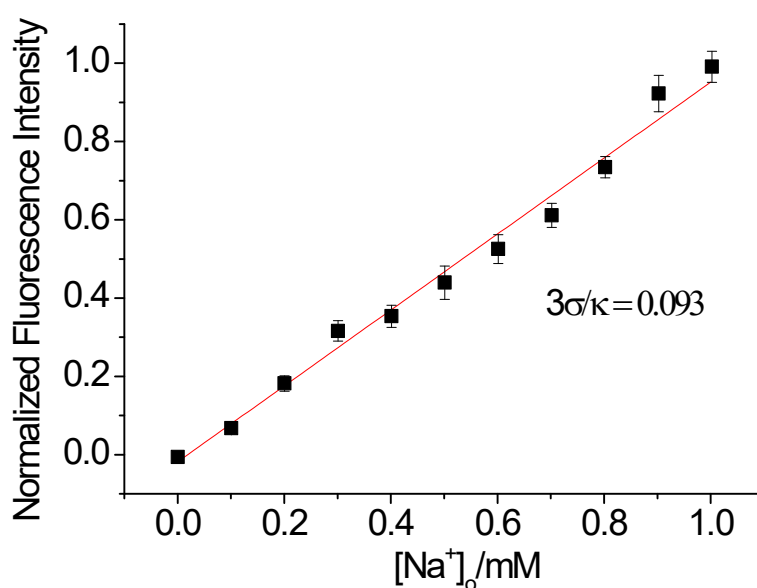
Figure S5. Plot of the fluorescence intensity for **CCNa1** versus [Na⁺] in MOPS buffer (10 mM MOPS, pH 7.0). The detection limit (93 ± 3 μM) was calculated with 3σ/k; where σ is the standard deviation of blank measurements and k is the slop in Figure S6. The excitation wavelength was 530 nm.
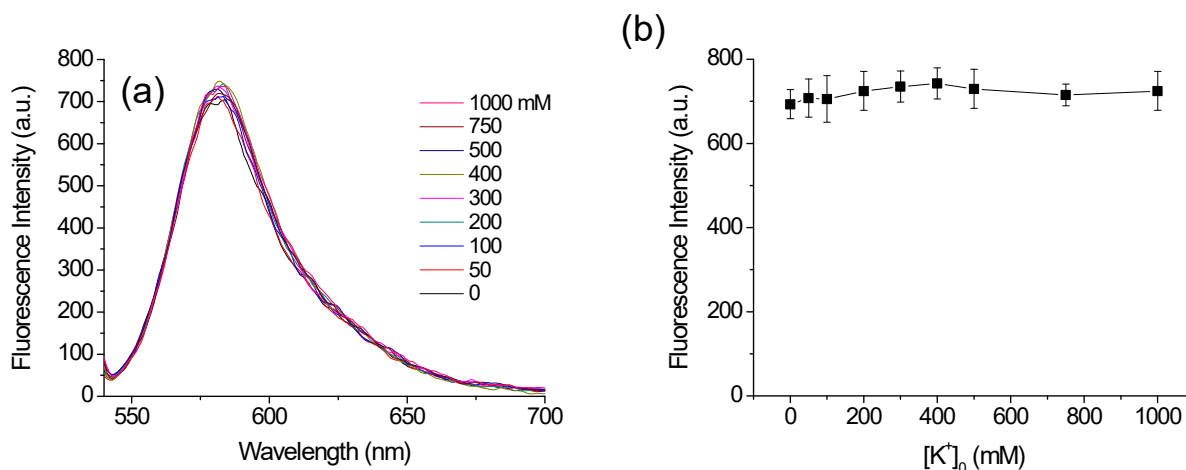
Figure S6. (a) One-photon emission spectra and for the complexation of 1 μM **CCNa1** (10 mM MOPS, pH 7.0) with free K^+ (0−1000 mM). (b) Titration curve for the complexation of 1 μM **CCNa1** (10 mM MOPS buffer, pH 7.0) with free K^+ (0-1000 mM). The solid line is the calculated values (Eq 2 and Ref.1). The emission spectra were recorded with λ_{Ex} = 530 nm.

**Measurement of Two-Photon Cross Section.** The two-photon cross section (δ) was determined by using femto second (fs) fluorescence measurement technique as described.[20] **CCNa1** (1.0×10^{-6} M) was prepared by dissolving in 10 mM MOPS buffer (500 mM NaCl, pH 7.0). The two-photon induced fluorescence intensity was measured between 720 and 940 nm by using rhodamine 6G as the reference.[21] When the reference and **CCNa1** were excited at the same excitation wavelength, the intensity of the two-photon induced fluorescence spectra were recorded. The TPA cross section was calculated by using Eq.3.

$$\delta = \delta_r(S_s\Phi_r\phi_r c_r)/(S_r\Phi_s\phi_s c_s)\ldots\ldots\ldots\ldots..(3)$$

where the subscripts s and r stand for the sample and reference, respectively. The intensity of the signal collected by a CCD detector was denoted as S. Φ is the fluorescence quantum yield. ϕ is the overall fluorescence collection efficiency of the experimental apparatus. The number density of the molecules in solution was denoted as c. δ_r is the TPA cross section of the reference molecule.
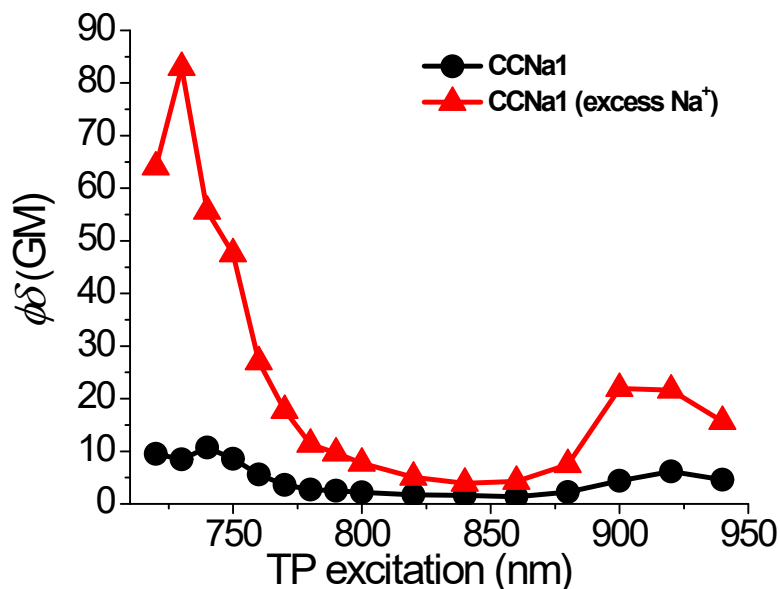
Figure S7. Two-photon action cross section (δΦ) value of 1 μM **CCNa1** (10 mM MOPS, pH 7.0) in the presence and absence of free Na^+.
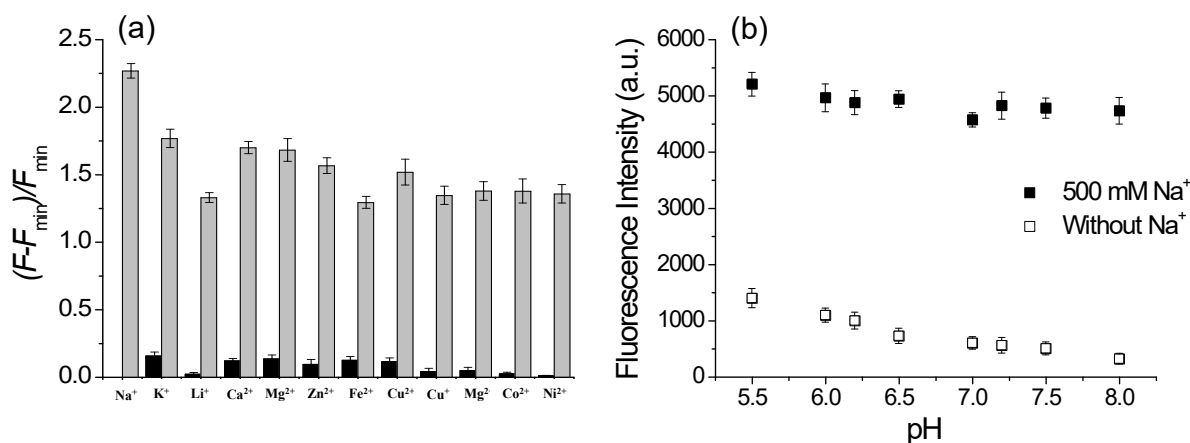

Figure S8. (a) The relative fluorescence intensity of **CCNa1** (10 mM MOPS, pH=7.0) in the presence of 200 mM for K^+, 5 mM Li^+, Ca^{2+}, Mg^{2+}; 100 μM for Zn^{2+}, Fe^{2+}, Cu^{2+}, Cu^+, Mn^{2+}, Co^{2+}, Ni^{2+} (■) and subsequent addition of 100 mM of Na^+ (■). (b) Effect of the pH on the one-photon fluorescence intensity of 1μM **CCNa1** in the presence of 0 (■) and 500 mM (■) of NaCl in 10 mM MOPS buffer. The emission was recorded with λ_{ex} = 530 nm.

Cell Culture. Primary astrocytes were cultured from the cortex of wild type mice brains. In brief, cortexes were removed and triturated in DMEM (Invitrogen, Carlsbad, CA, USA) containing 10% FBS (HyClone, Logan, UT, USA), plated in 75 cm² T-flasks (0.5 hemisphere/flask), and incubated for 2~3 weeks. Microglia were detached from flasks by mild shaking, filtered through a nylon mesh to remove cell clumps, and cultured in DMEM containing 10% FBS.[22] Astrocytes remaining in the flask were harvested with 0.1% trypsin and cultured in DMEM containing 10% FBS. BV2 murine microglia were cultured in DMEM containing 5% FBS as previously described.[23] For activation of glial cells,

cells were treated with 5 ng/ml recombinant murine IFN-γ (PeproTech, Rocky Hill, NJ, USA). After 7-15 days in vitro, astrocytes were washed three times with serum-free media, and then incubated with 1.0 μL of 1 mM **CCNa1** in DMSO stock solution (1.0 μM **CCNa1**) at 37 °C under 5 % CO_2 for 10 min.

Two-Photon Fluorescence Microscopy. Two-photon fluorescence microscopy images of CCNa1 labeled cells and tissues were obtained with spectral confocal and multiphoton microscopes (Leica TCS SP8 MP) with ×10 dry, ×40 oil, ×63 oil and ×100 oil objectives, numerical aperture (NA) = 0.30, 1.30, 1.40, and 1.30, respectively. The two-photon fluorescence microscopy images were obtained with a DMI6000B Microscope (Leica) by exciting the probe with a mode-locked titanium-sapphire laser source (Mai Tai HP; Spectra Physics, 80 MHz pulse frequency, 100 fs pulse width) set at wavelength 750 nm and output power 2510 mW, which corresponded to approximately 10 mW average power in the focal plane. To obtain images at 450-550 nm range, internal PMTs were used to collect the signals in an 8 bit unsigned 512 × 512 and 1024 × 1024 pixels at 400 and 200 Hz scan speed, respectively.
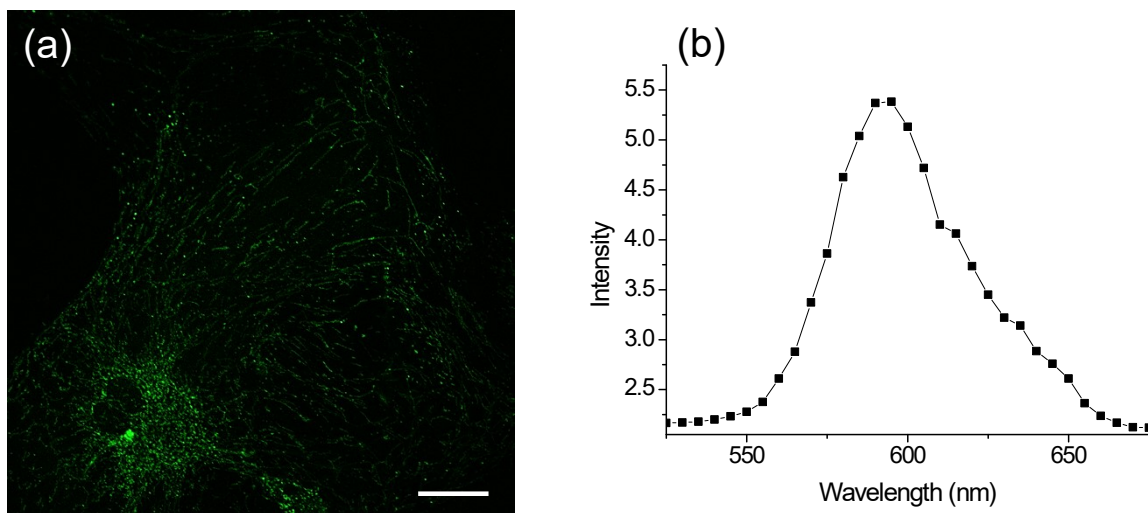

Figure S9. TPM images of **CCNa1** (1μM) (a) astrocytes collected at 450-695 nm (b) Two-photon excited fluorescence spectrum for astrocytes. The excitation wavelength was 730 nm

Photostability. The photostability of **CCNa1** was studied by monitoring the changes in TPEF intensity with time at four designated positions of **CCNa1** (1 μM) astrocytes cells chosen without bias (Figure S7b). The TPEF intensity remained nearly the same for 1 hr (Figures S7b), indicating the probe has high photostability.
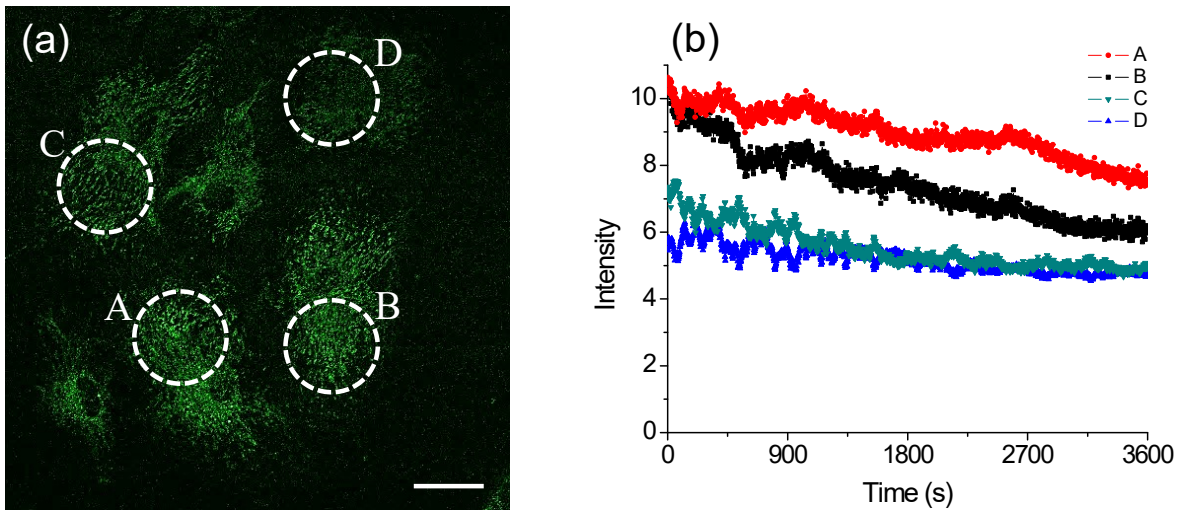

Figure S10. TPM images of **CCNa1** (1μM) (a) astrocytes collected at 450-695 nm. (b) The relative TPM intensity for astrocytes as a function of time. The digitized intensity was recorded with 2.00 sec intervals for 1 h using *xyt* mode with femto-second pulses. Cells shown are representative images from replicate experiments (n = 5), Scale bar 40 μm.
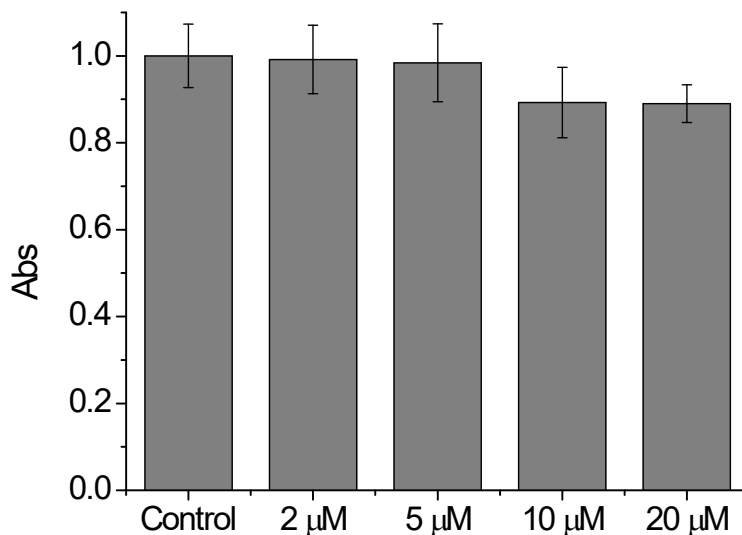

Figure S11. Viability of HeLa cells in the presence of **CCNa1** as measured by using MTS assay. The cells were incubated with Probe for 2 h.
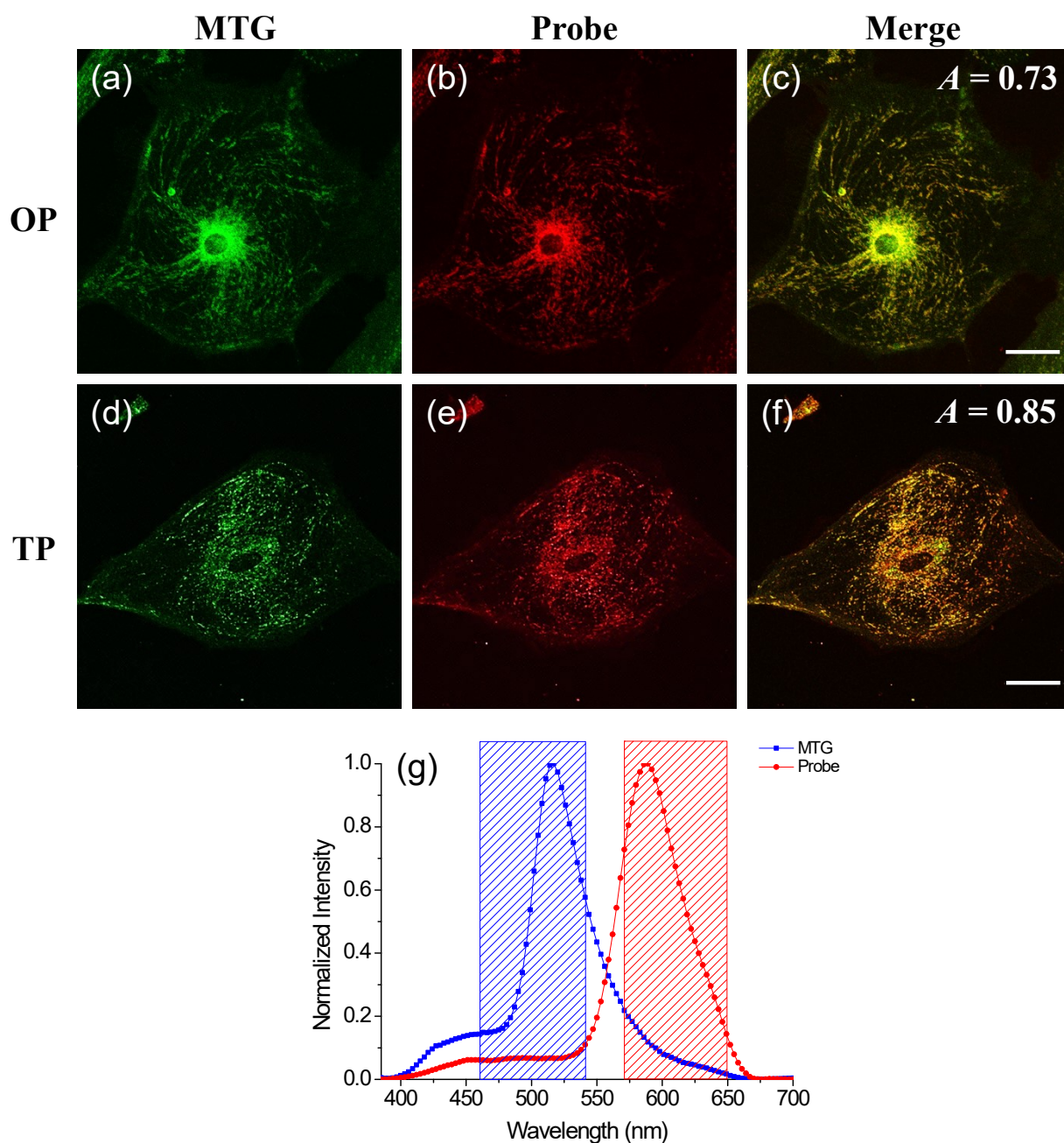
Figure S12. (a,b,c) OPM and (d,e,f) TPM images of astrocyte co-localized with MTG (a,d 1 µM) and **CCNa1** (b,e 2 µM) for 10 min 37 ºC. (c,f) Merged images. The wavelengths for OP and TP excitation were (a) 488, (b) 552 and (d,e) 740 nm respectively, and the corresponding emission were collected at (a) 495-545 nm, (b) 560-655 nm, (d) 460-540 nm, and (e) 570-650 nm. (g) two-photon excitied fluorescence spectra of MTG and **CCNa1** in astrocyte, and the detection windows for MTG (blue channel) and **CCNa1** (red channel) The image shown are representative of the images obtatined in the repeat experiments (n = 5). Scale bars : (c) 32 µm and (f) 48 µm.
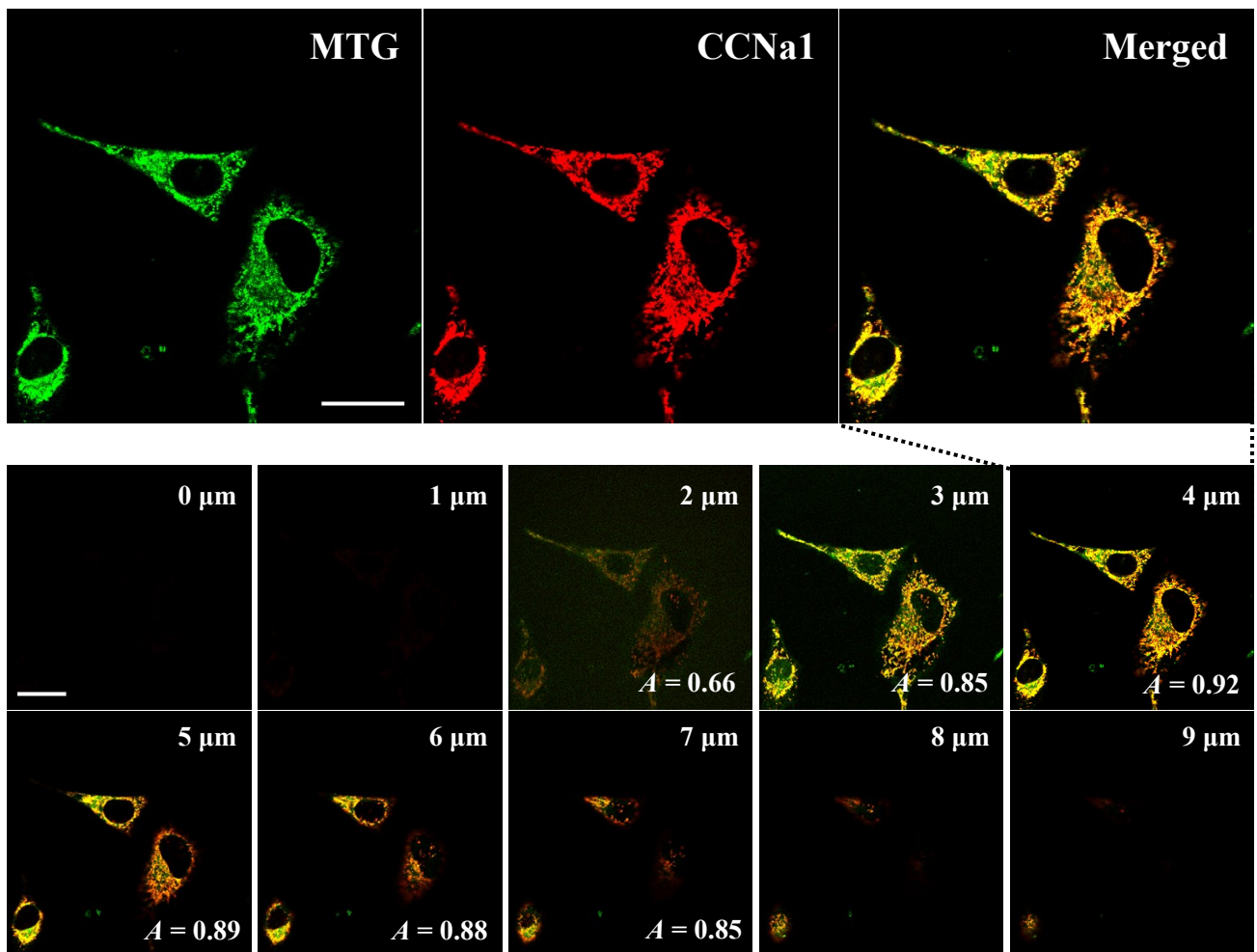
Figure S13. The z-sectional co-localization images of **CCNa1** with **MTG** in live HeLa cells. The excitation wavelength was 488 nm with the emission windows of 495–545 nm for MitoTracker Green (**MTG**), 560–655 nm for **CCNa1**, respectively. The above z-sectional images are representative images from replicated experiments (n = 5). Scale bars = 30 μm.
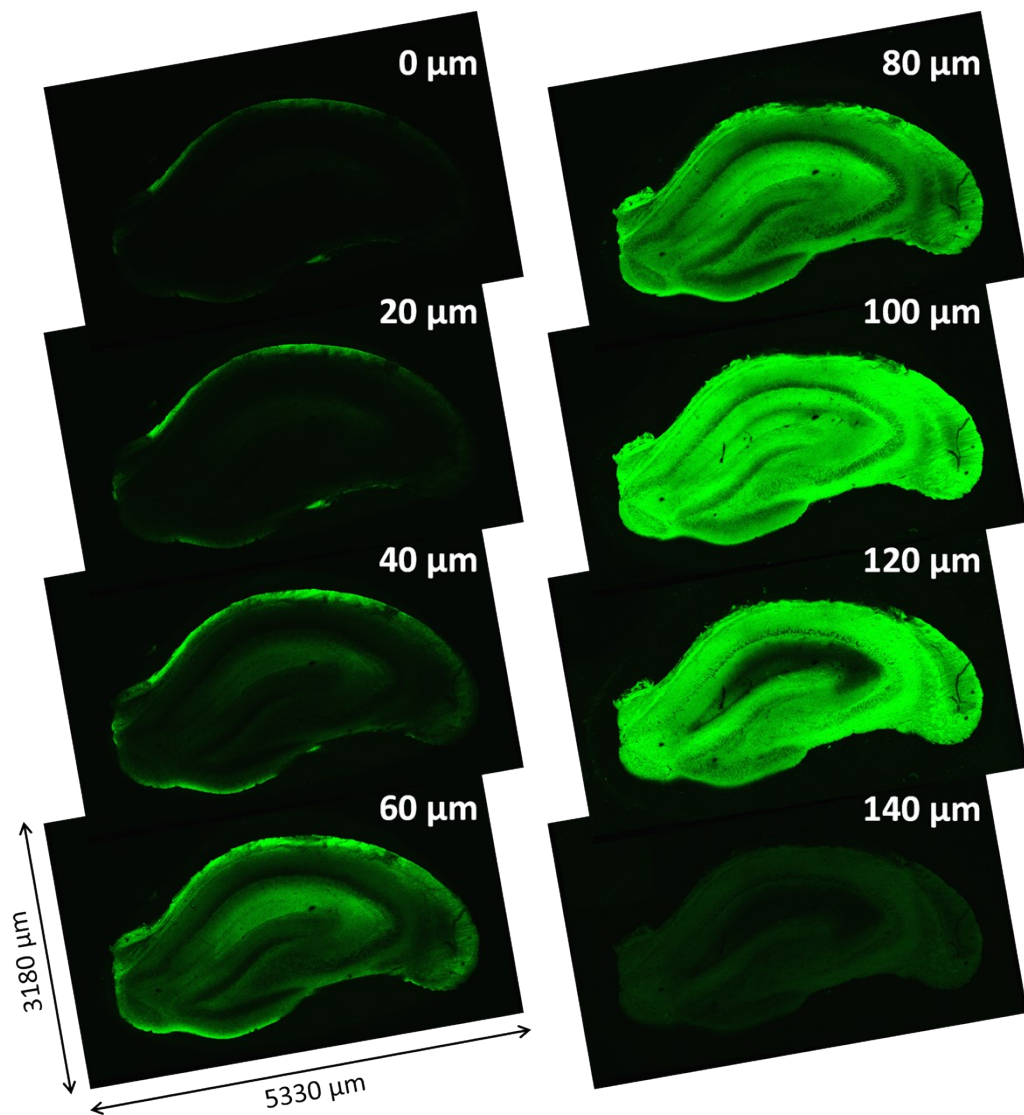
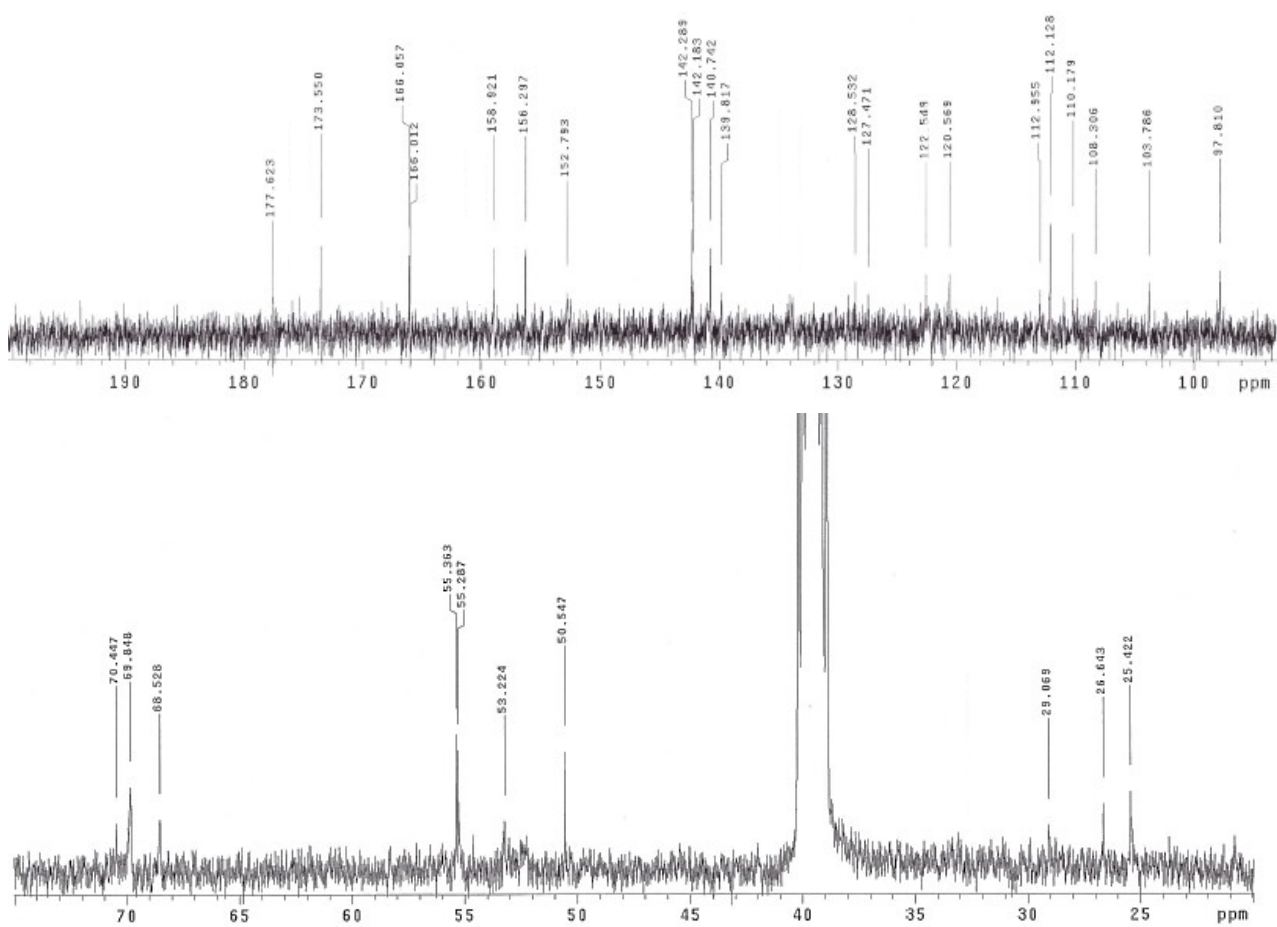**Figure S14.** The z-sectional TPM images of **CCNa1**-labeled mouse hippocampal slice. TP excitation wavelength was 730 nm with emission windows of 455–695 nm. The above z-sectional live tissue images are representative images from replicated experiments (n = 3).
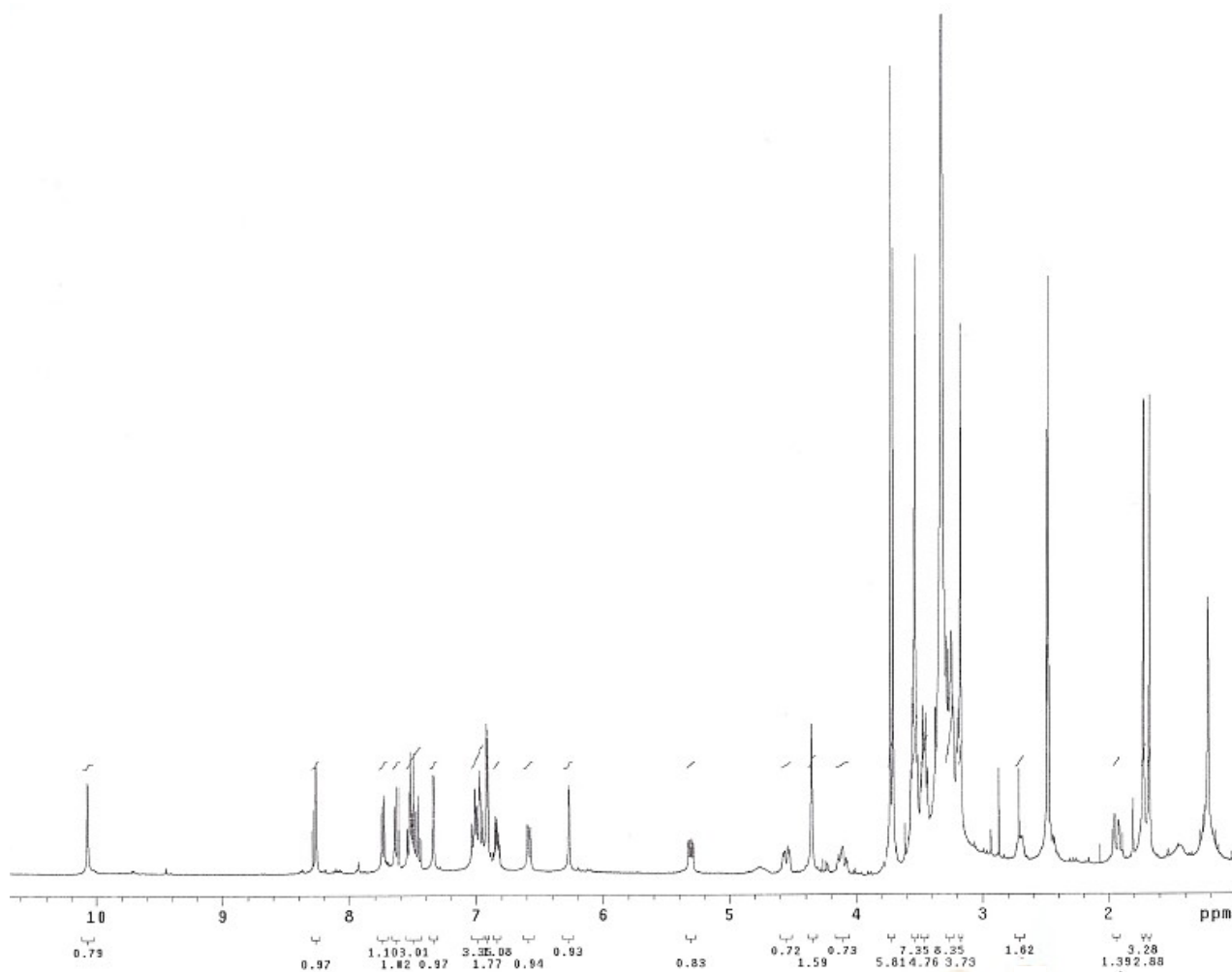
Figure S15. ^{1}H-NMR spectrum (400 MHz) of **CCNa1** in d6-DMSO.

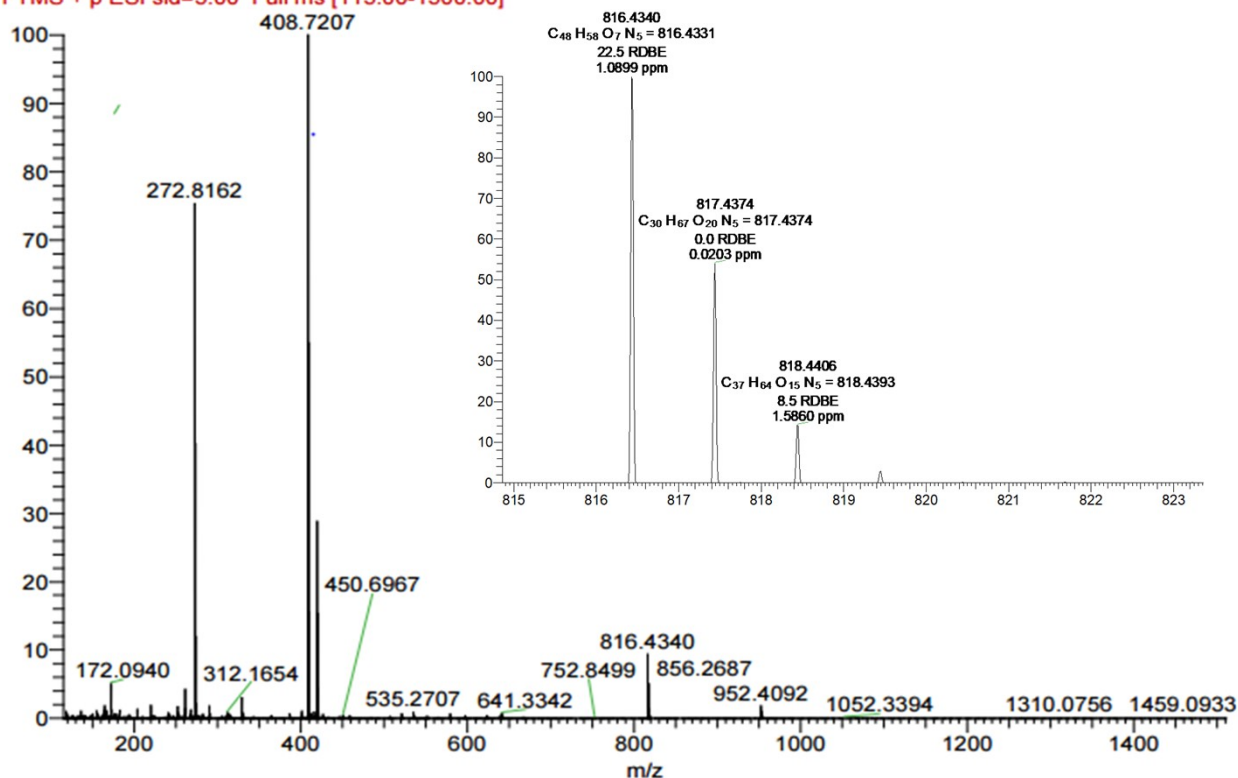**Figure S16.** ^{13}C-NMR spectrum (100 MHz) of **CCNa1** in d6-DMSO.

Figure S17. HRMS data of **CCNa1**

References

(1)   T. Gunnlaugsson, H. Q. N. Gunaratne, M. Nieuwenhuyzen and J. P. Leonard,   *J. Chem. Soc. Perk. T 1*, 2002, 1954.

(2)   H. M. Kim, H. J. Choo, S. Y. Jung, Y. G. Ko, W. H. Park, S. J. Jeon, C. H. Kim, T. Joo and B. R. Cho, *ChemBioChem*, 2007, **8**, 553

(3)   C. Reichardt, *Chem. Rev.*, 1994, **94**, 2319.

(4)   A. Minta and R. Y. Tsien, *J. Biol. Chem.*, 1989, **264**, 19449–19457.

(5)   H. M. Kim, C. Jung, B. R. Kim, S.-Y. Jung, J. H. Hong, Y. -G. Hong, J. -S. Park, K. J. Lee and B. R. Cho*, Angew. Chem., Int. Ed.*, 2007, **46**,   3460–3463.

(6)   H. Szmacinski and J. R. Lakowicz, *Anal. Biochem.*, 1997, **250**, 131–138.

(7)   P. Roder and C. Hille, *Photochem. Photobiol. Sci.*, 2014, **13**(12), 1699–1710.

(8)   M. Kollmannsberger, K. Rurack, U. Resch-Genger, W. Rettig and J. Daub, *Chem. Phys. Lett.*, 2000, **329**, 363.

(9)   V. V. Martin, A. Rothe, Z. Diwu and K. R. Gee, *Bioorg. Med. Chem. Lett.*, 2004, **14**, 5313–5316.

(10)   M. Taki, H. Ogasawara, H. Osaki, A. Fukazawa, Y. Sato, K. Ogasawara, T. Higashiyama and S. Yamaguchi, *Chem. Commun.*, 2015, **51**, 11880–11883.

(11)   T. Schwarze, H. Müller, D. Schmidt, J. Riemer and H. Holdt, *Chem.–Eur. J.*, 2017, **23**, 7255–

7266.

(12)   A. R. Sarkar, C. H. Heo, M. Y. Park, H. W. Lee and H. M. Kim, *Chem. Commun*., 2014, **50**, 1309-1312.

(13)   M. J. Frisch, G. W. Trucks, H. B. Schlegel, G. E. Scuseria, M. A. Robb, J. R. Cheeseman, G. Scalmani, V. Barone, G. A. Petersson, H. Nakatsuji, X. Li, M. Caricato, A. V. Marenich, J. Bloino, B. G. Janesko, R. Gomperts, B. Mennucci, H. P. Hratchian, J. V. Ortiz, A. F. Izmaylov, J. L. Sonnenberg, Williams, F. Ding, F. Lipparini, F. Egidi, J. Goings, B. Peng, A. Petrone, T. Henderson, D. Ranasinghe, V. G. Zakrzewski, J. Gao, N. Rega, G. Zheng, W. Liang, M. Hada, M. Ehara, K. Toyota, R. Fukuda, J. Hasegawa, M. Ishida, T. Nakajima, Y. Honda, O. Kitao, H. Nakai, T. Vreven, K. Throssell, J. A. Montgomery Jr., J. E. Peralta, F. Ogliaro, M. J. Bearpark, J. J. Heyd, E. N. Brothers, K. N. Kudin, V. N. Staroverov, T. A. Keith, R. Kobayashi, J. Normand, K. Raghavachari, A. P. Rendell, J. C. Burant, S. S. Iyengar, J. Tomasi, M. Cossi, J. M. Millam, M. Klene, C. Adamo, R. Cammi, J. W. Ochterski, R. L. Martin, K. Morokuma, O. Farkas, J. B. Foresman and D. J. Fox, Gaussian 09, Revision C.01, 2010.

(14)   R. L. Martin, *J. Chem. Phys*., 2003, **118**, 4775-4777.

(15)   R. Dennington, T. A. Keith and J. M. Millam, GaussView, Version 5.0, 2009.

(16)   W. Liu, C. Fan, R. Sun, Y.-J. Xu and J.-F. Ge, *Org. Biomol. Chem*., 2015, **13**, 4532-4538.

(17)   T. Yanai, D. P. Tew and N. C. Handy, *Chem. Phys. Lett*., 2004, **393**, 51-57.

(18)   A. Minta and R. Y. Tsien, *J. Biol. Chem.*, 1989, **264**, 19449. B

(19)   (a) J. R. Long and R. S. Drago, *J. Chem. Ed.*, 1982, 59, 1037; (b) K. Hirose, *J. Incl. Phenom. Macrocycle. Chem.*, 2001, **39**, 193.

(20)   S. K. Lee, W. J. Yang, J. J. Choi, C. H. Kim, S. J. Jeon and B. R. Cho, *Org. Lett.*, 2005, **7**, 323.

(21)   C. Xu and W. W. Webb, *J. Opt. Soc. Am. B,* 1996, **13**, 481.

(22)   H. Pyo, I. Jou, S. Jung, S. Hong and E. H. Joe, *Neuroreport*, 1998, **9**, 871.

(23)   K. J. Min, I. Jou and E. Joe, *Biochem. Biophys. Res. Commun.*, 2003, **312**, 969.